



Biogeochemical Variability of the Upper Ocean Response to Typhoons and Storms in the Northern South China Sea

Yung-Yen Shih^{1,2}, Chin-Chang Hung^{2*}, Szu-Yu Huang², François L. L. Muller² and Yu-Hsuan Chen¹

¹ Department of Applied Science, R.O.C Naval Academy, Kaohsiung, Taiwan, ² Department of Oceanography, National Sun Yat-sen University, Kaohsiung, Taiwan

OPEN ACCESS

Edited by:

Jianfang Chen,
Second Institute of Oceanography,
Ministry of Natural Resources, China

Reviewed by:

Glen Gawarkiewicz,
Woods Hole Oceanographic
Institution, United States
Kuanbo Zhou,
Xiamen University, China

*Correspondence:

Chin-Chang Hung
cchung@mail.nsysu.edu.tw

Specialty section:

This article was submitted to
Marine Biogeochemistry,
a section of the journal
Frontiers in Marine Science

Received: 04 November 2019

Accepted: 27 February 2020

Published: 20 March 2020

Citation:

Shih Y-Y, Hung C-C, Huang S-Y,
Muller FLL and Chen Y-H (2020)
Biogeochemical Variability of the
Upper Ocean Response to Typhoons
and Storms in the Northern South
China Sea. *Front. Mar. Sci.* 7:151.
doi: 10.3389/fmars.2020.00151

Satellite remote sensing of chlorophyll *a* (Chl) has produced evidence of typhoon-induced phytoplankton blooms in the tropical and subtropical ocean but it is difficult to evaluate if the particulate organic carbon (POC) fixed by marine organisms can be transported into deep waters. Recent field observations have shown enhancements in primary production, Chl and POC flux associated with the passage of typhoons over the shallow waters (<200 m) of the continental shelf. However, it is still unclear whether typhoons, which originate beyond the continental margin, can transfer the newly fixed carbon to deeper waters. Here we report on nitrate + nitrite (N), Chl and POC fluxes in the northern South China Sea (NSCS) before and shortly after the passage of typhoons and storms, between September 2012 and June 2014. The integrated inventories of N (0–150 m) 8, 3, 2, and 5 days after the passage of typhoons *Tembin*, *Soulik*, and *Knongrey* were 0.44, 0.16, 0.36, and 0.48 mol m⁻², and these values were not significantly different from inventories of N under normal, non-typhoon conditions (0.18 ~ 0.48 mol m⁻²). The integrated Chl values 8, 3, 2, and 5 days after the passage of typhoons *Tembin*, *Soulik*, and *Knongrey* were 35, 24, 14, and 28 mg m⁻², i.e., lower than Chl inventories when no typhoons occurred (29 ~ 40 mg m⁻²). POC fluxes after the passage of typhoons *Tembin* and *Soulik* were 78 ± 12 and 115 ± 16 mg-C m⁻² d⁻¹ (average ± 1 standard deviation), i.e., 1.6 and 2.4 times higher than those obtained before the typhoon. In addition, variations in both surface and depth-integrated Chl were decoupled from POC fluxes. This decoupling may be attributed to a change in the plankton community composition due to water column instability or to lateral inputs of particulate matter released from shelf or slope sediments. Overall, our analysis of this 2-year dataset highlights the spatial and temporal variability of the factors controlling POC exports to the deep NSCS.

Keywords: typhoon, nutrient, chlorophyll, carbon flux, northern South China Sea

INTRODUCTION

Concentrations of chlorophyll *a* (Chl) at the ocean surface represent the status of marine planktonic phototrophs that contribute to the biological pump. Export fluxes of particulate organic carbon (POC) to the ocean's interior have been used extensively to assess the strength of this “biological pump.” Enhanced Chl and abundant phytoplankton biomass which is able to take up more CO₂ by

photosynthesis and move the fixed organic carbon to the deep ocean. The POC export flux from the upper ocean (i.e., euphotic zone) to the deep ocean is one of the key mechanisms controlling the partial pressure of CO₂ in surface waters of the ocean over time (Emerson et al., 1997; Lin et al., 2003; Tseng et al., 2005; Hung et al., 2010). Both Chl concentrations and POC fluxes are therefore important to understand the oceanic carbon cycle and evaluate future scenarios for global climate change (Emerson et al., 1997; Siswanto et al., 2007). Due to the challenges of working at sea in stormy weather, accurate measurements of Chl and POC during a typhoon or storm are currently lacking (Hung et al., 2010; Hung and Gong, 2011; Chen et al., 2013, 2015; Shih et al., 2015).

Typhoons, also known as tropical cyclones or hurricanes, normally originate from the low-latitude ocean; they generally travel longer distances over the open ocean than across shallow waters during their life span. As they progress from coastal waters to land, their structure and strength weaken rapidly. Previous work in shallow waters has demonstrated that typhoons are able to cause dramatic hydrographic as well as biogeochemical responses [e.g., cooling of the sea surface, enhancement and deepening of primary production and increased export of POC (Chang et al., 1996; Shiah et al., 2000; Hung et al., 2010; Hung and Gong, 2011; Chung et al., 2012; Shih et al., 2015)]. These effects are well documented in situations where typhoons have passed over shallow waters (Siswanto et al., 2007; Chen et al., 2009; Shih et al., 2013) but the impact of typhoons on the ocean's biological pump and carbon export to the deep ocean remain unclear. To date, the only documented examples of typhoons causing significant vertical mixing, stimulating biogeochemical activity and leading to efficient carbon sequestration below the euphotic zone and export to the deep ocean (>1000 m) have been in the oligotrophic northwestern Pacific Ocean (Chen et al., 2009, 2013; McGee and He, 2018).

Representing 90% of the global surface ocean, the open ocean accounts for 82% and 80% of the global oceanic primary production and organic carbon removal, respectively (Martin et al., 1987); it is an essential part of the global carbon cycle. The open ocean also includes all known areas of typhoon formation. Once formed, typhoons can travel long distances over open waters where their interactions with the upper ocean have yet to be fully elucidated. Although satellite remote sensing data show evidence of cooling, deepening of the mixed layer and increased biological activity following the passage of a typhoon (Lin et al., 2003; Babin et al., 2004; Zheng and Tang, 2007), remote sensing techniques still have limitations over cloudy or rough seas and in areas influenced by colored dissolved organic matters (CDOM) (Shang et al., 2008; Hung et al., 2010).

The South China Sea (SCS) is the world's largest marginal sea (Hung et al., 2007) and it is also one of the world's sea areas most frequently visited by typhoons (Chen et al., 2015). The northern SCS (NSCS), especially the northeastern part, is a major corridor for effective seawater exchange between warm SCS seawater and western north Pacific seawater (Liu et al., 2002). The NSCS has subtrophic and oligotrophic characteristics, i.e., the surface Chl concentration is low ($\sim 0.1 \text{ mg m}^{-3}$), the subsurface Chl maximum lies at or above the nitracline depth

(Z_{NO₃}) and the concentration of nitrate + nitrite (N) above the nitracline is near or below detection limit (Liu et al., 2002; Zheng and Tang, 2007). Therefore, the NSCS is an excellent region to study the effects of typhoons on biogeochemical responses in a warm and oligotrophic open ocean.

In this study, we conducted 14 cruises in the NSCS from 2012 to 2014, covering all seasons and capturing the passage of 3 typhoons (wet season) and 4 storms (dry season). Each cruise comprised a visit to a fixed sampling station, which allowed us to study the temporal variability in the upper ocean biological responses to typhoons and storms at that location.

MATERIALS AND METHODS

The 14 cruises were conducted aboard the R/V *Ocean Researcher III* (OR-III) and V (OR-V) from September 2012 to June 2014. Station H (22.0°N 120.3°E, water depth $\sim 1000 \text{ m}$), located approximately 70 km southwest of Taiwan (Figures 1a,c; station H1 at Figure 1b, 20.3°N 120.3°E, water depth $\sim 3600 \text{ m}$, 270 km southwest of Taiwan, was selected only for typhoon *Soulik*), was occupied on all cruises to provide a 2-year time series. Four of these expeditions took place a few days after passages of typhoons: *Tembin* (24–28 August 2012, moderate intensity, wind gusts: 35–45 m s⁻¹, maximum sustained wind: 21 m s⁻¹), *Soulik* (11–13 July 2013, severe intensity, wind gusts: 51 m s⁻¹, maximum sustained wind: 11 m s⁻¹) and *Kongrey* (27–29 August 2013, mild intensity, wind gusts: 25 m s⁻¹, maximum sustained wind: 8 m s⁻¹) (satellite images of typhoon impact are shown in Supplementary Figure S1). Daily average precipitation associated with typhoons *Tembin*, *Soulik*, and *Kongrey* are 24 (1–68), 14 (1–29), and 107 (1–308) mm, respectively. These typhoons did a lot of damage on the southwestern seaboard of Taiwan due to torrential rain, as recorded by the Central Weather Bureau of R.O.C. (CWB)¹. Four other cruises took place shortly after storms (wind speed $\geq 17 \text{ m s}^{-1}$; 29 October, 1 December 2012; 14 April, 13 October 2013). Data showing average daily precipitation (Pingtung station, P, 22.7°N 120.5°E) as well as river discharge (Liling station, L, 22.8°N 120.4°E) by the Gaoping River were provided by the Water Resources Agency of R.O.C. (WRA)². Wind speed and wave height were recorded at the Eluanbi buoy (120.8°E 21.9°N) by the CWB. The wave height data for 1 December 2012 was obtained from the relationship: Wave Height = 0.09 × Wind Speed + 0.30, $r = 0.51$, $p < 0.01$, $n = 98$. Sampling events were labeled as “typhoon” or “storm” if they took place within 8 days of a passage of a typhoon or storm. It is worth noting that all typhoons occurred in the wet season (June–September) while all storms occurred in the dry season (October–May). By extension, we use the terms “non-typhoon” and “non-storm” to designate those sampling events that occurred during wet season (25 September 2012, 9 September 2013, 24 June 2014) and dry season

¹www.cwb.gov.tw

²www.wra.gov.tw

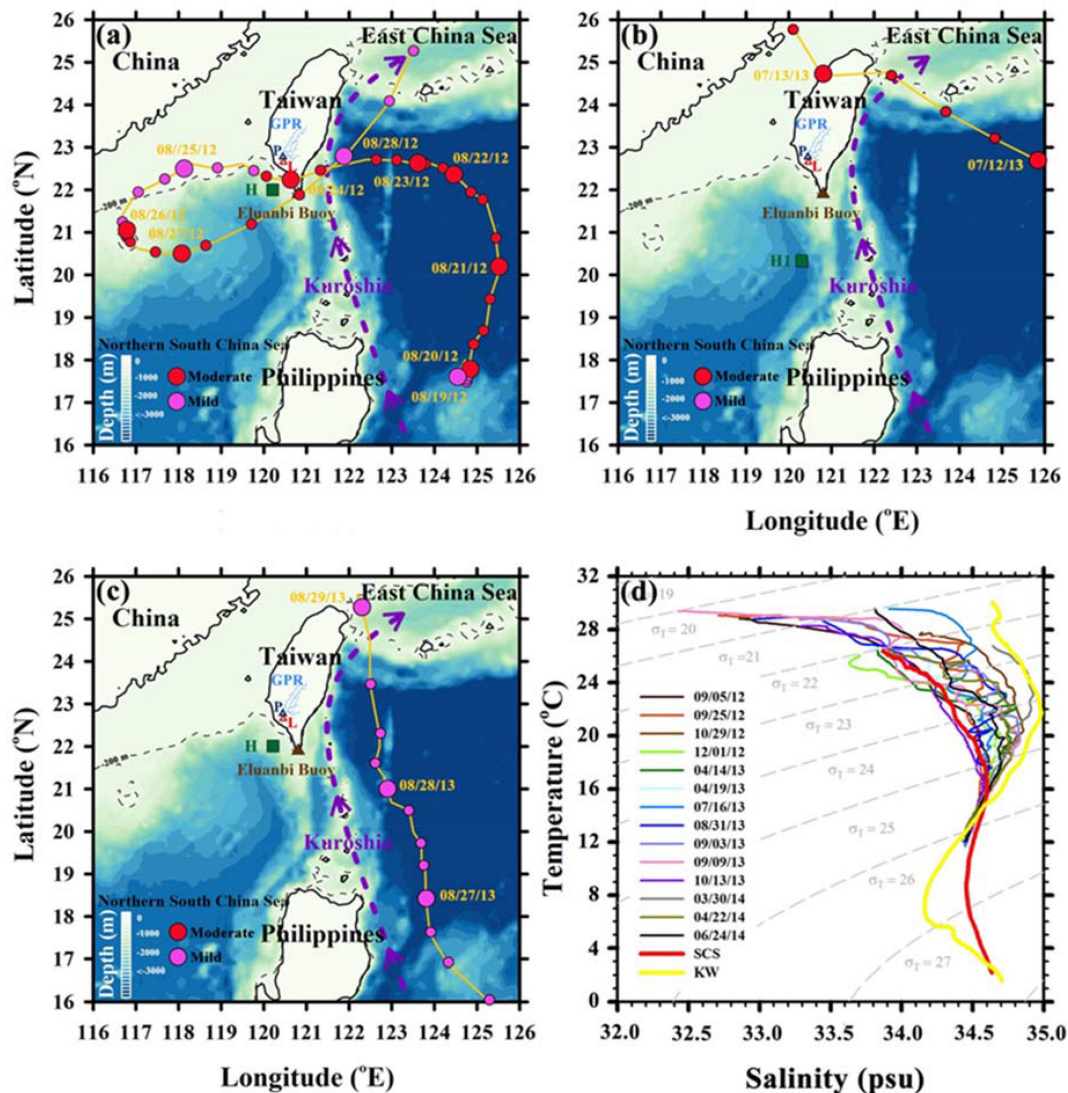


FIGURE 1 | The maps show the tracks of typhoon *Tembin* (a), *Soulik* (b), and *Kongrey* (c). The 14 temperature-salinity profiles (d) are for the upper 300 m of the water column at station H (13 sampling events) or H1 (1 sampling event, i.e., typhoon *Soulik*) between September 2012 and June 2014. For each typhoon, tracking (light yellow line) was initiated at 06:00 LMT on the start date (larger circle symbol) and then plotted at 6-h intervals (smaller circle symbol) using red or pink solid circles depending on typhoon intensity at the time. The dash purple line represents Kuroshio Current. The abbreviations GPR, P and L over southern Taiwan stand for Gaoping River, Pingtung rain gauge, and Liling river discharge station, respectively.

background conditions (19 April 2013, 30 March 2014, 22 April 2014), respectively.

Seawater temperature, density and salinity were measured using a CTD sensor (SBE 911 plus mode, SeaBird Scientific Inc.). The mixed layer depth (MLD) was defined by the temperature-based criterion of a 0.8°C decrease from the surface (Kara et al., 2000; Shih et al., 2015). Nitrate + nitrite was analyzed by flow injection analysis according to Gong et al. (1995a). Water samples for Chl analysis were immediately filtered through 25-mm GF/F filters and stored frozen at -20°C until analysis. The Chl retained on the filter was extracted by acetone and measured according to standard procedures using a Turner Designs 10AU-005 fluorometer by the non-acidification method

(Gong et al., 1995b; Hung et al., 2010). Sediment trap samples for POC analysis were resuspended with filtered seawater and then filtered through pre-combusted quartz filters ($1.0\ \mu\text{m}$ pore size). Following rinsing and drying of the filters, POC was measured with a CHN analyzer following fuming with concentrated HCl in a desiccator to remove PIC (Hung and Gong, 2010). Inventories of N (I-N), Chl (I-Chl), and POC (I-POC) were calculated for the upper 150 m. For the cruises conducted on 19 April, 3 September 2013, and 22 April 2014, we used relationships: $[\text{Chl}] = 2.29 \times \text{Fluorescence Intensity} - 0.01$, $r = 0.89$, $p < 0.01$, $n = 87$; $[\text{N}] = 25.72 - 0.94 \times \text{Temperature}$, $r = 0.91$, $p < 0.01$, $n = 79$ (Supplementary Figure S2), to obtain vertical profiles of Chl and N. The depth of the nitracline (Z_{NO_3}) was determined

as the depth at which N equaled $1 \mu\text{M}$ (Reynolds et al., 2007). Remotely sensed surface Chl values were obtained from the website of CoastWatch directly³. We used Aqua MODIS daily level-3 products (4 km resolutions). If we could not find the daily data, the 8-days data (16 Jul and 13 October 2013) or no data (14 April, 31 August and 3 September 2013) were then selected or decided upon.

Sinking particles were collected at 150 m using a drifting sediment trap. This collection depth lay beneath the euphotic zone depth, i.e., where the photosynthetically active radiation had dropped to 1% of its surface value. The period of deployment was typically 24–36 h, but less than 24 h if the sea state made shipboard conditions untenable. After recovery of the trap, we used forceps to carefully remove swimmers on filter papers under a microscope. POC fluxes were then determined using the procedures described in detail in Hung et al. (2010) and Hung and Gong (2010). The retention time (RT, days) of POC in the upper 150 m of the water column was obtained by dividing I-POC (g m^{-2}) by the POC flux at 150 m ($\text{g m}^{-2} \text{d}^{-1}$).

RESULTS

Hydrographic and Weather Data

To compare long-term observed records (34.5 ± 12.3) from years 2008 to 2017, the daily average rain amount related to typhoons was as much as ~ 4 and ~ 23 times higher than the wet and dry seasons (9.1 ± 4.7 and $1.5 \pm 0.6 \text{ mm day}^{-1}$), respectively (Supplementary Figure S3). Apparently, the heavy rain amount is a substantial factor of the typhoon impact on the ocean. The temperature-salinity (T-S) profiles are shown in Figure 1d. They result from the mixing of warm SCS water with Kuroshio water (KW). The lowest surface salinity (5 m depth) was observed on 9 September 2013, i.e., 11 days after the passage of typhoon *Kongrey*. At densities below 23 kg m^{-3} , T-S properties very occasionally fell outside the domain defined by the SCS and KW. This might be due to processes such as precipitation or river runoff which decreased surface salinity (Supplementary Figures S4–S6).

Within 8 days of the passage of typhoon *Tembin*, wind speed and wave height went from maximum values of 19.3 m s^{-1} and 3.8 m to less than 10.0 m s^{-1} , and 1.0 m, respectively (Figure 2). For typhoons *Soulik* and *Kongrey*, the maximum values (wind speed, wave height) were (13.7 m s^{-1} , 2.1 m) and (18.3 m s^{-1} , 3.5 m), respectively. The average temperature of the mixed layer (T_{ML}) for these typhoons ranged from 28.7 to 29.2 (average = 28.8°C) for typhoon events, i.e., slightly lower than during the remainder of the wet season (28.9–29.3, average = 29.1°C , Figure 2). The mean MLD (35–58) m for typhoons was correspondingly a bit deeper than for wet-season non-typhoon conditions (20–65, average: 45 m, Figure 2). It should also be pointed out that much of the rainfall during the wet season actually came from typhoons. Highest daily precipitation was reported during and after the passage of typhoons *Kongrey*, followed by *Tembin* and *Soulik* (~ 230 ,

~ 60 , and $\sim 30 \text{ mm}$, respectively, Figure 2). Highest discharge values of the Gaoping River (GPR) were ~ 1100 , ~ 470 , and $\sim 370 \text{ m}^3 \text{ s}^{-1}$ for respective typhoons *Kongrey*, *Soulik*, and *Tembin* (Figure 2). The corresponding surface salinity minima that were subsequently recorded at the station were 32.42 on 9 September 2013, 32.74 on 25 September 2012, and 32.89 on 5 September 2012.

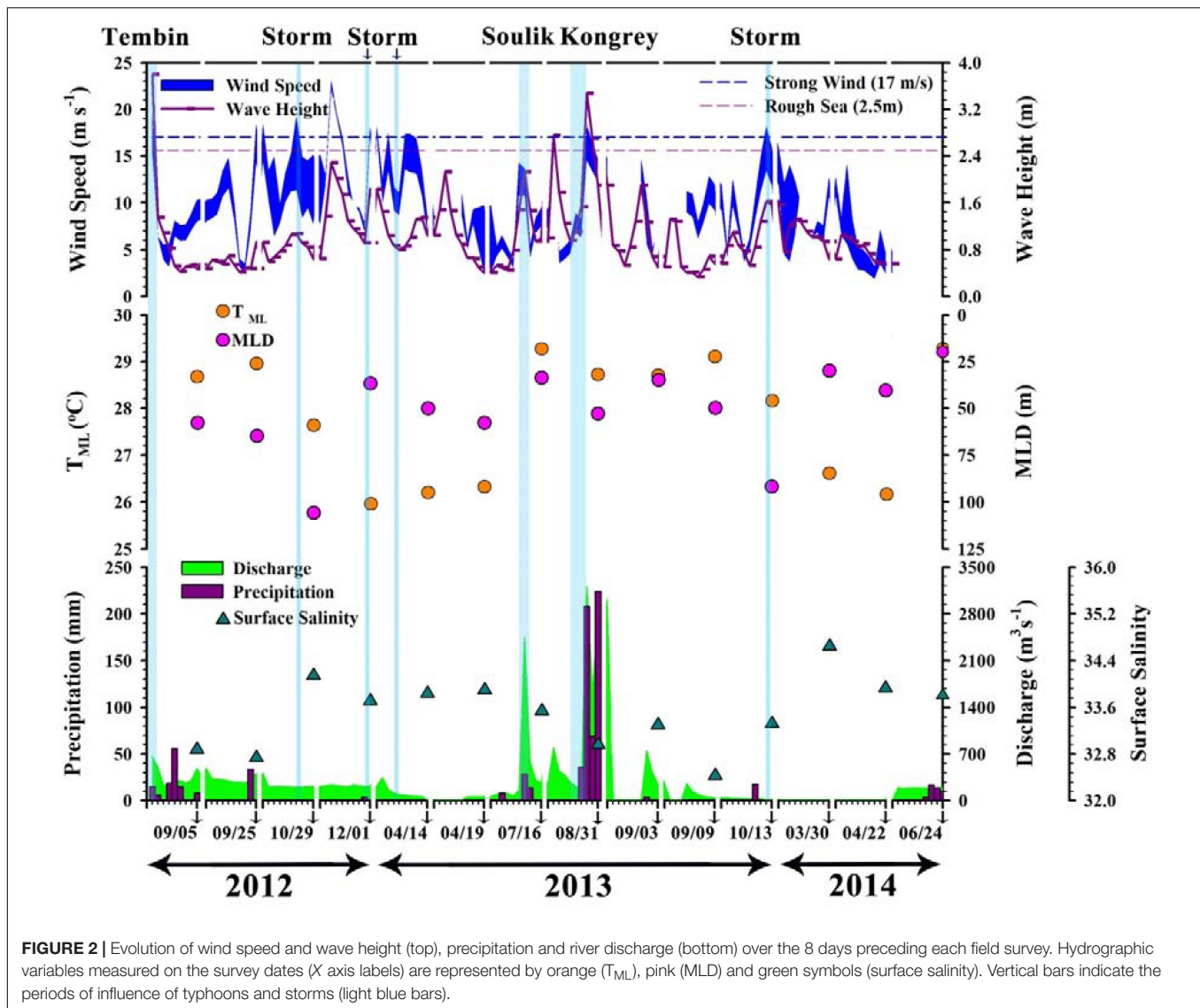
Storm events, which were all associated with the northeast monsoon, were defined as episodes of high wind (close to or above 15 m s^{-1}) lasting for several days to a week (Figure 2). Although a maximum wind speed of 23 m s^{-1} was recorded on 24 November 2012, 7 days before our sampling event, wind speed steadily decreased to 8 m s^{-1} until 1 December 2012; it then gusted up to 18 m s^{-1} to produce a second storm. The highest average wave height (1.5 m) occurred during the second storm (on 1 December 2012), followed by other storm events on 4 April 2013, 13 October 2013, and 29 October 2012 (average wave height: 1.1, 1.0, and 0.8 m, Figure 2). The MLD deepened from 30–58 m (average = 43 m) under dry-season, non-storm conditions to 37–106 m (average = 71 m) after the passage of the storms. Surprisingly, this was not accompanied by cooling of the surface water. Indeed, T_{ML} values were very similar under non-storm conditions (26.2–26.6; average $T_{\text{ML}} = 26.4^\circ\text{C}$) as under stormy conditions (25.9–28.2; average $T_{\text{ML}} = 27.0^\circ\text{C}$). The high surface salinity values observed just after the storms (33.32–34.14) and indeed throughout most of the dry season (33.90–34.64) were typical of the northeast monsoon climate of southwest Taiwan (Hung and Huang, 2005).

Vertical Distributions of N, Chl, and POC

Vertical profiles of N showed typical surface water depletions and gradual enrichments with increasing depths (Figure 3). Surface water N concentrations became readily detectable after the passages of typhoons *Soulik* and *Kongrey* ($0.2\text{--}0.4 \mu\text{M}$), storms ($0.3\text{--}0.8 \mu\text{M}$, 29 October and 01 December 2012), and at various times during the dry season ($0.1\text{--}0.8 \mu\text{M}$, 30 March and 22 April 2014). During the wet season, the combination of heavy rainfall and high river discharge from the Gaoping River contributed to detectable levels of N in the surface waters as well as to depressed salinity values of 32.74 on 25 September 2012 and 32.42 on 9 September 2013 (Figure 2). The average depth of the nitracline was greatest under wet-season background weather conditions ($Z_{\text{NO}_3} = 48\text{--}107$; average = 82 m). No consistent trend was observed when progressing from dry-season non-storm conditions (8–118; 62 m) through storm (44–117; 79 m) to full-on typhoon conditions (44–107; 76 m). This suggests that the combination of steady winds and lower temperatures prevailing in the dry season (Tseng et al., 2005; Liu et al., 2007; Hung et al., 2013a) had as much effect on Z_{NO_3} as typhoons.

Vertical concentration profiles of Chl and POC concentrations showed a similar pattern for most cruises, suggesting that the POC was associated with phytoplankton biomass. The average surface Chl levels showed no systematic variations between typhoons ($0.05\text{--}0.31$, average = 0.15 mg m^{-3}), wet-season non-typhoon conditions ($0.10\text{--}0.17$, average: 0.13 mg m^{-3}), storms ($0.12\text{--}0.23$, average: 0.15 mg m^{-3}) and dry-season non-storm conditions ($0.07\text{--}0.29$, average: 0.16 mg m^{-3}). A prominent

³<https://coastwatch.pfeg.noaa.gov>



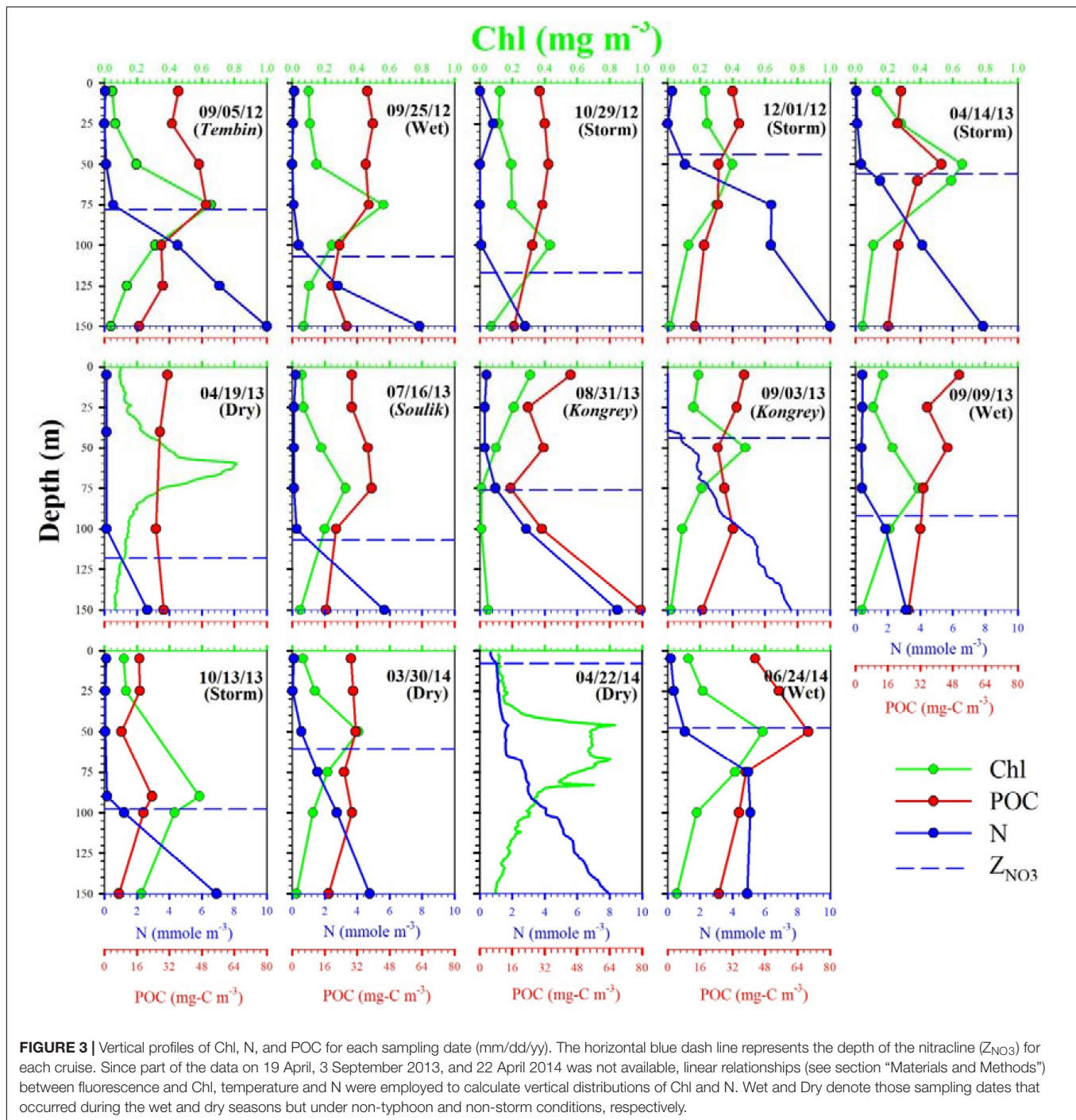
subsurface Chl maximum was observed between depths 40 and 100 m with the highest concentration (0.8 mg m^{-3}) in the dry season (19 April 2013 and 22 April 2014). It lay at or close to Z_{NO_3} suggesting that N supply had stimulated new primary production at those depths (Moloney et al., 1991; Hung et al., 2009b). Elevated Chl concentrations also appeared at the sea surface 2 days after the passage of typhoon *Kongrey* (31 August 2013). This was a transient phenomenon which was attributed to the instability of the upper ocean water column (Hung et al., 2010) induced by this typhoon.

Vertical POC profiles exhibited concentrations in the range $9\text{--}69 \text{ mg-C m}^{-3}$ generally with decreasing trends in the upper 100 m. Below that depth, POC decreased to lower values ($7\text{--}29 \text{ mg-C m}^{-3}$) for most cruises, apart from the relatively large deep maximum at 79 mg-C m^{-3} observed 2 days after typhoon *Kongrey* on 31 August 2013 (Figure 3). The concentration of POC at the depth of 150 m is higher than that in the upper ocean. It implies that materials of POC at lower depth cannot be predicted

by a 1-D biological vertical degradation pattern. The underlying driving force between POC and interacted mechanisms may be ignored. This remarkable feature of POC may be attributed to lateral off-shelf transport of resuspended material just after typhoons (Hung et al., 2013b; Shih et al., 2019).

Inventories (I-N, I-Chl and I-POC), POC Fluxes and Retention Time

The one-dimensional water column inventory of N (I-N) showed no noticeable seasonal variations, but it was higher during typhoons and storms ($0.16\text{--}0.48$, average = 0.36 mol m^{-2} ; $0.09\text{--}0.69$, average = 0.36 mol m^{-2}) than at any other times of the wet and dry seasons ($0.18\text{--}0.48$, average = 0.28 mol m^{-2} ; $0.08\text{--}0.49$, average = 0.28 mol m^{-2} ; Figure 4A). By contrast, the Chl inventory (I-Chl) was actually lower in the wake of typhoons ($14\text{--}35$, average = 25 mg m^{-2}) than at other times (storms: $32\text{--}41$, average = 36 mg m^{-2} ; wet-season: $29\text{--}40$, average = 34 mg



m^{-2} ; dry-season: 25–49, average = 36 $mg\ m^{-2}$; **Figure 4B**). The average I-POC after typhoons (4.8 $g-C\ m^{-2}$) and storms (3.4 $g-C\ m^{-2}$) showed lower values compared with the background I-POC values recorded in the wet season (5.5 $g-C\ m^{-2}$) and dry season (4.1 $g-C\ m^{-2}$), respectively (**Figure 4C**).

Particulate organic carbon export fluxes shortly after typhoons averaged 97 (78–115) $mg-C\ m^{-2}\ d^{-1}$ which was higher than that at any other time of the wet season (42–73, average = 58 $mg-C\ m^{-2}\ d^{-1}$). Likewise, the mean export flux of POC associated with

storms (54–95, average = 80 $mg-C\ m^{-2}\ d^{-1}$) was greater than that of any other time of the dry season (44–74, average = 59 $mg-C\ m^{-2}\ d^{-1}$, **Figure 4D**). These higher export fluxes meant that the retention times of POC associated with post-typhoons and storms (37–69, average = 53 days; 25–65, average = 45 days, **Figure 4E**) were shorter than during the remainder of the wet season (90–112, average = 101 days) and dry season (55–94, average = 75 days), respectively. These results are consistent with the notion that typhoons and storms can efficiently trigger

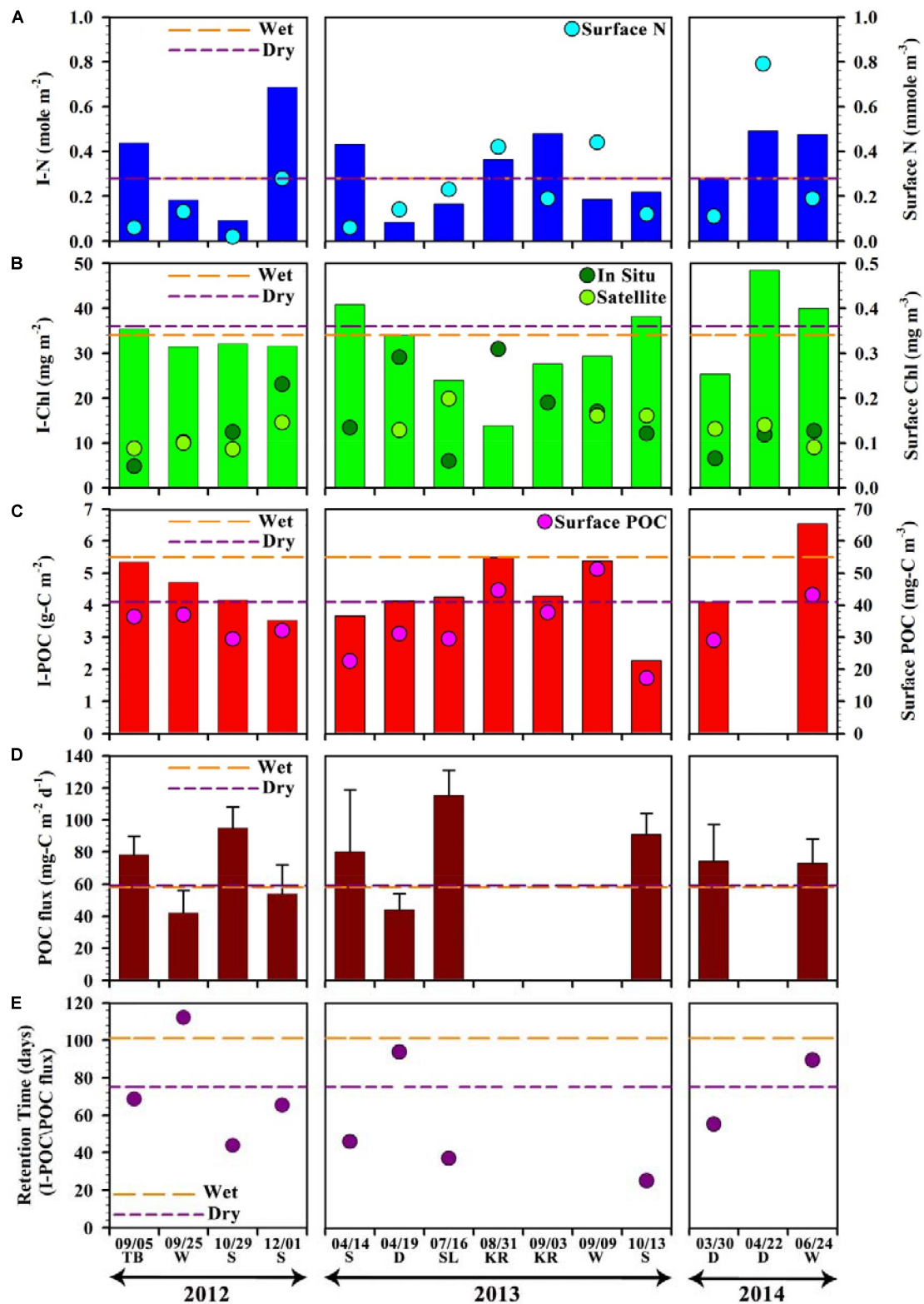


FIGURE 4 | Integrated (0–150 m) and surface values of N (A), Chl (B), and POC (C) are shown for each of the 14 sampling dates. POC fluxes (D) were measured at 150 m depth, i.e., below the euphotic zone; thus retention times (E) represent the fractional residence times of POC in the upper 150 m with respect of settling out of particulate organic matter. Dashed lines represent average values in the wet (orange) and dry (purple) seasons. TB, SL, KR, S, D, and W stand for typhoons *Tembin*, *Soulik*, *Kongrey*, storms, dry, and wet seasons, respectively.

elevated POC fluxes from the upper layer to the deeper ocean in the warm oligotrophic NSCS.

DISCUSSION

N Entrainment After Passages of Typhoons and Storms

Depth-integrated N concentrations increased by $0.53 \mu\text{M}$ [$(0.36\text{--}0.28) \text{ mol m}^{-2}/150 \text{ m} = 0.00053 \text{ mol m}^{-3}$] and $0.48 \mu\text{M}$ [$(0.36\text{--}0.28) \text{ mol m}^{-2}/150 \text{ m} = 0.00048 \text{ mol m}^{-3}$] after the passage of a typhoon or storm, respectively (see section “Inventories (I-N, I-Chl and I-POC), POC Fluxes and Retention Time”). The increase was mainly due to intense upwelling generated by Ekman pumping (Chen and Tang, 2012; Jan et al., 2017) and/or turbulent mixing caused by these very strong wind events (Hung et al., 2009b, 2010). Additionally, the contribution of terrestrial inputs of N should not be ignored (Chen et al., 2009; Chung et al., 2012; Hung et al., 2013a) since surface salinity minima and detectable surface N concentrations (greater than the general detection limit $0.1 \mu\text{M}$, **Figure 3**) were observed after the passage of typhoons *Kongrey*, *Soulik*, and *Tembin*.

It was noteworthy that POC inventories decreased after the passage of a typhoon or storm. The average decrease was from 5.5 to 4.8 g-C m^{-2} in the wet season and from 4.1 to 3.4 g-C m^{-2} in the dry season. This implied the POC was withdrawn from the upper 150 m of the water column. Assuming that POC fluxes held up for as long as the physical forcing of typhoons (7 days) or storms (10 days) persisted (Hung et al., 2010; Chu and Chang, 2012), these fluxes would have been 100 and $70 \text{ mg-C m}^{-2} \text{ day}^{-1}$ which is close to the average fluxes previously reported for typhoons and storms (97 and $80 \text{ mg-C m}^{-2} \text{ day}^{-1}$, respectively). The amount of N associated with this lost POC must therefore be factored into the calculation of the turbulent flux of N into the upper 150 m . The changes in POC concentration was 0.7 g-C m^{-2} in both typhoon and storm events. Using a C/N ratio of 6.625 (Redfield et al., 1963), this change would thus result in a change of 0.06 ($0.7 \text{ g-C m}^{-2}/150 \text{ m}/12 \text{ g-C mol}^{-1}/6.625$) μM in N. To compensate for this loss, total additions of N into the upper 150 m water column were consequently 0.59 ($0.53 + 0.06$) and 0.54 ($0.48 + 0.06$) μM after typhoons and storms, respectively. Although these two values were considerably less than the $6.77 \mu\text{M}$ (N) reported by Hung et al. (2010) in the shelf area (water depth $<200 \text{ m}$) of southern East China Sea, they were sufficient to stimulate biological activity in the oligotrophic oceanic province of the NSCS.

Implications of Reduced Chl Inventories (I-Chl) After Typhoons and Storms

With the exception of typhoon *Tembin*, where the I-Chl value was slightly higher (35 mg m^{-2}) than during non-typhoon conditions (31 mg m^{-2}), typhoon I-Chl values were generally depressed compared to wet-season background conditions. For example, I-Chl values were 14 and 28 mg m^{-2} 2 and 5 days after the passage of typhoon *Kongrey*, as compared to a wet-season average of 29 mg m^{-2} . This low stock of Chl phenomenon

can be interpreted as follows: the entrainment of colder and fresher water (**Figure 2**) into the upper column creates a perturbation for phytoplankton cells that are in their early growth phase and perhaps initiate a shift toward a different phytoplankton assemblage (see explanation in next section). Overall, the integrated Chl values were significantly higher pre-typhoon than post-typhoon (34 vs. 25 mg m^{-2}). Similar results were also recorded in the dry season, i.e., higher I-Chl values for pre-storm than post-storm sampling events (44 vs. 36 mg m^{-2}). This observation was not in agreement with the findings of Hung et al. (2009b, 2010) who reported that I-Chl after typhoon and strong northeast monsoon events were ~ 2.8 and ~ 1.6 times higher than those recorded during no typhoons and strong wind occurrences, respectively.

Clearly, it is difficult to unravel the physical and biogeochemical processes that act to increase or decrease I-Chl following a typhoon or storm (Sweeney et al., 2003). Water stability, light intensity, cloud cover, etc., which exhibit high variability during the life span of a typhoon, can all influence phytoplankton biomass and community structure (Chen et al., 2009; Hung et al., 2010; Chung et al., 2012). Therefore, it is not surprising if temporal variations of different frequencies can result in either lower (Chen et al., 2013; this study) or higher (Chen et al., 2009; this study) I-Chl values in typhoons than in normal conditions. One of the key determinants of I-Chl may be the balance struck between pico- or nanoplanktonic algal species and their microplanktonic counterparts. Low nutrient availability, which prevails in the NSCS under normal conditions, favors the smaller algal species because their higher surface-to-volume ratios and smaller diffusion layer thicknesses make them better at taking up nutrients. By contrast, higher nutrient availability, which occurs after the passage of a typhoon, is required to sustain the growth of the larger algal species. This may partly explain why the abundance of nitrogen-fixing (*Trichodesmium*, *R. intracellulare*, *unicellular cyanobacteria*) and small phytoplankton species (*Prochlorococcus*, *Synechococcus*) decreased by a factor of 4 under the nutrient-replete conditions occurring after typhoons in the vicinity of the Kuroshio (Chen et al., 2009). At the same time, the cell density of micro-sized phytoplankton (i.e., diatoms) had grown about eight times after these typhoons (Chen et al., 2009). Another example occurred 3 days after typhoon *Morakot*'s passage: Chung et al. (2012) pointed out that as I-Chl decreased to $\sim 31\%$ of its initial value there was a tenfold decrease in nitrogen-fixing cyanobacteria and small dinoflagellates but a 180-fold increase in large diatoms.

Besides the relationship between Chl and phytoplankton species composition, the slope of POC against Chl has also been reported as an important index to estimate carbon sources in different spatial and temporal conditions (Chang et al., 2003; Hung et al., 2009a). The average slope in our study was much lower than those reported by Hung et al. (2009a) (0.9 and $1.3\text{--}5.8 \text{ mol-C g-Chl}^{-1}$, respectively) in the East China Sea (ECS), suggesting that POC production came from different phytoplankton assemblages than in the NSCS. As a result, the I-Chl values measured in the NSCS after typhoons and storms show a dissimilar pattern compared to that in the ECS.

In summary, the direction and magnitude of the change in I-Chl after a typhoon or storm would seem to depend on the magnitude of the shift from pico- and nanoplanktonic species to microplanktonic species. We tested this hypothesis on our own experimental observations. For example, I-Chl was 31 mg m^{-2} on 25 September 2012 (wet season) but rose to 35 mg m^{-2} after typhoon *Tembin*. Assuming the Chl contribution of small phytoplankton was 87 (82–91)% and that of the large ones was 13 (9–18)% (Chen, 2000; Kameda and Ishizaka, 2005), it follows that small and large phytoplankton contributed 27 and 4 mg m^{-2} of Chl, respectively, during non-typhoon conditions. We then conservatively assumed that the biomass of small phytoplankton cells reduced to 50% (14 mg m^{-2}); the biomass of large phytoplankton would have had to increase at least five times (21 mg m^{-2}) after the typhoon. This is in reasonable agreement with our observation that the biomass of large phytoplankton cells increased on average 2.5 times after typhoons and 3.4 times after storms.

Implications of Shorter Retention Times After Typhoons and Storms

Typhoons and storms showed elevated POC fluxes (97 and $80 \text{ mg-C m}^{-2} \text{ d}^{-1}$) compared with those under wet-season and dry-season background conditions (58 and $59 \text{ mg-C m}^{-2} \text{ d}^{-1}$). The retention time of POC in the upper 150 m of the water column was shorter for typhoons and storms (53 and 45 days) than for other time periods of the wet and dry seasons (101 and 75 days). In other words, the average sinking velocity of these organic particles was greater in typhoons and storms (3.1 and 3.7 m d^{-1}) than prior to typhoons and storms (1.5 and 2.1 m d^{-1}). Furthermore, sinking velocities of the POC for typhoons and storms were close to the values of $3\text{--}5 \text{ m d}^{-1}$ reported by Huisman and Sommeijer (2002) for the microalgae *Gonyaulax* and *Coscinodiscus*. This is consistent with the point we made in section “Implications of Reduced Chl Inventories (I-Chl) After Typhoons and Storms” that the injection of nutrients into the euphotic zone causes phytoplankton to bloom and that the large-celled species (microphytoplankton) are better able to take advantage of this pulse of nutrients to increase their biomass.

Besides the sinking velocity, we examined the temporal variations in the ratio I-POC/I-Chl to evaluate the relative contributions from large and small phytoplankton. The lowest ratio was found to be associated with storm events (98) followed by dry-season non-storm (117), wet-season non-typhoon (166), and typhoons (243). These results suggest that seasonal changes occur between wet and dry seasons, possibly due to changes in the dominant phytoplankton species. The ratio for storm events (98) was similar to the upper limit (80) of values reported by Liu et al. (2007) for large phytoplankton cells. The ratio observed in typhoons is considered to be representative of the contribution of detritus and/or small phytoplankton aggregates through direct or indirect routes (Liu et al., 2007; Richardson and Jackson, 2007). In this case, more carbon may be exported to the deep ocean following resuspension of shelf sediments and lateral transport after the typhoon's passage (Shih et al., 2019). This external POC flux can be measured in deep waters (Shih et al., 2019). In

summary, our POC flux measurements support our contention that small phytoplankton and detritus make a large contribution to the elevated POC flux triggered by typhoons while large phytoplankton are largely responsible for the elevated POC flux caused by storms.

It is worth noting that although the one-dimensional POC flux was greater for typhoons than for storms, the duration and impact area of storms were much greater than for typhoons (Chen et al., 2013) so that the actual amount of carbon exported to the deep by storms may have been greater.

Decoupling Between Surface and Integrated N, Chl and POC

Due to the difficulties of deploying instrumentation over the side of a ship in heavy seas, surface sampling and/or satellite remote sensing are generally used instead to evaluate the oceanic biogeochemical response to a strong wind event (Lin et al., 2003; Shih et al., 2015). Here we found very significant differences between satellite measurements of surface Chl (aqua MODIS level 3 products) and our field measurements. For example, our measured surface Chl concentrations after the passage of typhoons *Tembin* and *Soulik* were 0.05 and 0.06 mg m^{-3} were much lower than satellite derived values (0.09 and 0.20 mg m^{-3}) suggesting that satellite-derived Chl values after typhoons might be overestimated due to possible interferences from non-pigment colored dissolved organic matter and/or suspended particles originating either from detritus or non-living materials.

In addition, we found no discernable correlations among the measured variables, i.e., N, I-N, surface Chl (*in situ* and satellite), I-Chl, surface POC and I-POC, however, did not correlate with each other (Figure 4). For instance, we found the highest surface N ($0.8 \mu\text{M}$) on 22 April 2014 but the highest I-N value (0.69 mol m^{-2}) was observed on 01 December 2012; the highest *in situ* surface Chl (0.31 mg m^{-3}) was observed on 31 August 2013, while the lowest I-Chl (14 mg m^{-2}) was recorded on that date; a low surface Chl (0.06 mg m^{-3}) was determined on 16 July 2013 while the highest surface Chl (0.20 mg m^{-3}) retrieved from the satellite occurred on that day. It was clear that variations in surface Chl were totally decoupled from variations in I-Chl.

This decoupling between surface and integrated N, Chl, and POC may have been caused by a number of factors. We have already mentioned the potential role for nutrients in structuring the planktonic ecosystem due to larger cells requiring a sustained supply of N. Another factor which is particularly relevant in oligotrophic regions, where Chl shows a maximum near the nitracline (Figure 3), is that the Chl maximum represents an adaptation to low solar irradiance and therefore is a poor indicator of phytoplankton biomass (Mignot et al., 2014). Further, it takes time for the water column to restabilize after the passage of a typhoon, so that the ecosystem structure is constantly evolving; therefore our sampling events may have captured a slightly different stage in the ecosystem's response to the perturbation. Finally, the intensity of the upwelling and vertical mixing induced by a typhoon in a given location is thought to increase with increasing wind speeds and decreasing translation velocity of the typhoon itself (Zhao et al., 2008).

This may explain why stronger, slow-moving typhoons tend to produce intense phytoplankton blooms which can be picked up by remotely sensed Chl measurements (Lin et al., 2003; Shang et al., 2008; Hung et al., 2010; Hung and Gong, 2011; Shih et al., 2013; Zhao et al., 2015). Differences in the intensity and translation velocity among the typhoons described here may thus account for some of the variability in the biogeochemical response at our sampling location.

The passage of a typhoon triggers a multitude of changes in the upper ocean which occur on time scales of hours, days or weeks as a result of nutrient pulses, phytoplankton and bacterial production and particle settling, respectively. There remain considerable challenges in describing these changes at a fixed location at different stages of a typhoon's passage. In the future, mesocosm studies (Stewart et al., 2013) and oceanic observational studies with data buoys (Jan et al., 2017) may help provide the high-frequency temporal data sets needed to resolve the biogeochemical and physical factors, respectively.

DATA AVAILABILITY STATEMENT

The raw data supporting the conclusions of this article will be made available by the authors, without undue reservation, to any qualified researcher.

REFERENCES

- Babin, S. M., Carton, J. A., Dickey, T. D., and Wiggert, J. D. (2004). Satellite evidence of hurricane-induced phytoplankton blooms in an oceanic desert. *J. Geophys. Res.* 109:C03043. doi: 10.1029/2003JC001938
- Chang, J., Chung, C. C., and Gong, G. C. (1996). Influences of cyclones on chlorophyll a concentration and *Synechococcus* abundance in a subtropical western Pacific coastal ecosystem. *Mar. Ecol. Prog. Ser.* 140, 199–205. doi: 10.3354/meps140199
- Chang, J., Shiah, F. K., Gong, G. C., and Chiang, K. P. (2003). Cross-shelf variation in carbon-to-chlorophyll a ratios in the East China Sea, summer 1998. *Deep Sea Res. II* 50, 1237–1247. doi: 10.1016/S0967-0645(03)00020-1
- Chen, K. S., Hung, C. C., Gong, G. C., Chou, W. C., Chung, C. C., Shih, Y. Y., et al. (2013). Enhanced POC export in the oligotrophic northwest Pacific Ocean after extreme weather events. *Geophys. Res. Lett.* 40, 5728–5734. doi: 10.1002/2013gl058300
- Chen, X., Pan, D., Bai, Y., He, X., Chen, C. T. A., Kang, Y., et al. (2015). Estimation of typhoon-enhanced primary production in the South China Sea: a comparison with the Western North Pacific. *Cont. Shelf Res.* 111, 286–293. doi: 10.1016/j.csr.2015.10.003
- Chen, Y., and Tang, D. (2012). Eddy-feature phytoplankton bloom induced by a tropical cyclone in the South China Sea. *Int. J. Remote Sens.* 33, 7444–7457. doi: 10.1080/01431161.2012.685976
- Chen, Y. L. L. (2000). Comparisons of primary productivity and phytoplankton size structure in the marginal regions of southern East China Sea. *Cont. Shelf Res.* 20, 437–458. doi: 10.1016/S0278-4343(99)00080-81
- Chen, Y. L. L., Chen, H. Y., Jan, S., and Tuo, S. H. (2009). Phytoplankton productivity enhancement and assemblage change in the upstream Kuroshio after typhoons. *Mar. Ecol. Prog. Ser.* 385, 111–126. doi: 10.3354/meps08053
- Chu, C. R., and Chang, Y. F. (2012). Long-term surface wind speed trends over Taiwan between 1961–2008. *Meteor. Bull.* 49, 51–68.
- Chung, C. C., Gong, G. C., and Hung, C. C. (2012). Effect of typhoon morakot on microphytoplankton population dynamics in the subtropical Northwest Pacific. *Mar. Ecol. Prog. Ser.* 448, 39–49. doi: 10.3354/meps09490

AUTHOR CONTRIBUTIONS

C-CH conceived the idea. Y-YS and C-CH wrote the manuscript with contributions from FM, Y-YS, and S-YH. Y-HC performed the experiments and created the figures. Y-YS, C-CH, and FM revised the manuscript. All authors reviewed the manuscript.

FUNDING

This research was supported by the Ministry of Science and Technology (MOST, Taiwan, Grant Numbers: 107-2611-M-012-001 and 108-2611-M-012-001) of Taiwan and Department of Education of Taiwan.

ACKNOWLEDGMENTS

We appreciate the assistance given us by the crews of R/V OR-3 and R/V OR-5.

SUPPLEMENTARY MATERIAL

The Supplementary Material for this article can be found online at: <https://www.frontiersin.org/articles/10.3389/fmars.2020.00151/full#supplementary-material>

- Emerson, S., Quay, P., Karl, D., Winn, C., Tupas, L., and Landry, M. (1997). Experimental determination of the organic carbon flux from open-ocean surface waters. *Nature* 389, 951–954. doi: 10.1038/40111
- Gong, G. C., Liu, K. K., and Pai, S. C. (1995a). Prediction of nitrate concentration from two end member mixing in the southern East China Sea. *Cont. Shelf Res.* 15, 827–842. doi: 10.1016/0278-4343(94)00039-p
- Gong, G. C., Yang, W. R., and Chang, J. (1995b). In vivo fluorescence-derived chlorophyll a concentration in the southern East China Sea. *Acta Oceanogr. Taiwan.* 34, 73–85.
- Huisman, J., and Sommeijer, B. (2002). Maximal sustainable sinking velocity of phytoplankton. *Mar. Ecol. Prog. Ser.* 244, 39–48. doi: 10.3354/meps244039
- Hung, C. C., Chung, C. C., Gong, G. C., Jan, S., Tsai, Y. L., Chen, K. S., et al. (2013a). Nutrient supply in the Southern East China Sea after typhoon Morakot. *J. Mar. Res.* 71, 133–149. doi: 10.1357/002224013807343425
- Hung, C. C., Tseng, C. W., Gong, G. C., Chen, K. S., Chen, M. H., and Hsu, S. C. (2013b). Fluxes of particulate organic carbon in the East China Sea in summer. *Biogeosciences* 10, 6469–6484. doi: 10.1016/j.envpol.2018.11.059
- Hung, C. C., and Gong, G. C. (2010). POC/234Th ratios in particles collected in sediment traps in the northern South China Sea. *Estuar. Coast. Shelf Sci.* 88, 303–310. doi: 10.1016/j.ecss.2010.04.008
- Hung, C. C., and Gong, G. C. (2011). Biogeochemical responses in the Southern East China Sea after typhoons. *Oceanography* 24, 42–51. doi: 10.5670/oceanog.2011.93
- Hung, C. C., Gong, G. C., Chiang, K. P., Chen, H. Y., and Yeager, K. M. (2009a). Particulate carbohydrates and uronic acids in the northern East China Sea. *Estuar. Coast. Shelf Sci.* 84, 565–572. doi: 10.1016/j.ecss.2009.07.025
- Hung, C. C., Gong, G. C., Chou, W. C., Chung, C. C., Lee, M. A., Chang, Y., et al. (2010). The effect of typhoon on particulate organic carbon flux in the southern East China Sea. *Biogeosciences* 7, 3007–3018. doi: 10.5194/bg-7-3007-2010
- Hung, C. C., Gong, G. C., Chung, W. C., Kuo, W. T., and Lin, F. C. (2009b). Enhancement of particulate organic carbon export flux induced by atmospheric forcing in the subtropical oligotrophic northwest Pacific Ocean. *Mar. Chem.* 113, 19–24. doi: 10.1016/j.marchem.2008.11.004

- Hung, J. J., and Huang, M. H. (2005). Seasonal variations of organic-carbon and nutrient transport through a tropical estuary (Tsengwen) in southwestern Taiwan. *Environ. Geochem. Health* 27, 75–95. doi: 10.1007/s10653-004-2291-1
- Hung, J. J., Wang, S. M., and Chen, Y. L. (2007). Biogeochemical controls on distributions and fluxes of dissolved and particulate organic carbon in the Northern South China Sea. *Deep Sea Res. II* 54, 1486–1503. doi: 10.1016/j.dsr2.2007.05.006
- Jan, S. Y. J., Yang, H.-I., Chang, M.-H., and Wei, C.-L. (2017). New data buoys watch typhoons from within the storm. *Eos* 98, 24–27. doi: 10.1029/2017EO069821
- Kameda, T., and Ishizaka, J. (2005). Size-fractionated primary production estimated by a two-phytoplankton community model applicable to ocean color remote sensing. *J. Oceanogr.* 61, 663–672. doi: 10.1007/s10872-005-0074-7
- Kara, A. B., Rochford, P. A., and Hurlburt, H. E. (2000). An optimal definition for ocean mixed layer depth. *J. Geophys. Res.* 105, 16803–16821. doi: 10.1029/2000jc900072
- Lin, I., Liu, W. T., Wu, C. C., Wong, G. T. F., Hu, C. M., Chen, Z. Q., et al. (2003). New evidence for enhanced ocean primary production triggered by tropical cyclone. *Geophys. Res. Lett.* 30:1718. doi: 10.1029/2003gl017141
- Liu, K. K., Chao, S. Y., Shaw, P. T., Gong, G. C., Chen, C. C., and Tang, T. Y. (2002). Monsoon-forced chlorophyll distribution and primary production in the South China Sea: observations and a numerical study. *Deep Sea Res. I* 49, 1387–1412. doi: 10.1016/S0967-0637(02)00035-3
- Liu, K. K., Chen, Y. J., Tseng, C. M., Lin, I. I., Liu, H. B., and Snidvongs, A. (2007). The significance of phytoplankton photo-adaptation and benthic-pelagic coupling to primary production in the South China Sea: observations and numerical investigations. *Deep Sea Res. II* 54, 1546–1574. doi: 10.1016/j.dsr2.2007.05.009
- Martin, J. H., Knauer, G. A., Karl, D. M., and Broenkow, W. W. (1987). VERTEX: carbon cycling in the northeast Pacific. *Deep Sea Res.* 34, 267–285. doi: 10.1016/0198-0149(87)90086-0
- McGee, L., and He, R. (2018). Mesoscale and submesoscale mechanisms behind asymmetric cooling and phytoplankton blooms induced by hurricanes: a comparison between an open ocean case and a continental shelf sea case. *Ocean Dyn.* 68, 1443–1456. doi: 10.1007/s10236-018-1203-3
- Mignot, A., Claustre, H., Uitz, J., Poteau, A., D’Ortenzio, F., and Xing, X. (2014). Understanding the seasonal dynamics of phytoplankton biomass and the deep chlorophyll maximum in oligotrophic environments: a bio-argo float investigation. *Global Biogeochem. Cycles* 28, 856–876. doi: 10.1002/2013GB004781
- Moloney, C. L., Field, J. G., and Lucas, M. I. (1991). The size-based dynamics of plankton food webs. II. Simulations of three contrasting southern Benguela food webs. *J. Plankton Res.* 13, 1039–1092. doi: 10.1093/plankt/13.5.1039
- Redfield, A. C., Ketchum, B. H., and Richard, F. A. (1963). “The influence of organisms on the composition of sea water,” in *The Sea*, 2, ed. M. N. Hill, (New York, NY: Interscience), 26–77.
- Reynolds, S. E., Mather, R. L., Wolff, G. A., Williams, R. G., Landolfi, A., Sanders, R., et al. (2007). How widespread and important is N₂ fixation in the North Atlantic Ocean? *Glob. Biogeochem. Cycles* 21:GB4015. doi: 10.1029/2006GB002886
- Richardson, T. L., and Jackson, G. A. (2007). Small phytoplankton and carbon export from the surface ocean. *Science* 315, 838–840. doi: 10.1126/science.1133471
- Shang, S. L., Li, L., Sun, F. Q., Wu, J. Y., Hu, C. M., Chen, D. W., et al. (2008). Changes of temperature and bio-optical properties in the South China Sea in response to Typhoon Lingling, 2001. *Geophys. Res. Lett.* 35:L10602. doi: 10.1029/2008GL033502
- Shiah, F. K., Chung, S. W., Kao, S. J., Gong, G. C., and Liu, K. K. (2000). Biological and hydrographical responses to tropical cyclones (typhoons) in the continental shelf of the Taiwan Strait. *Cont. Shelf Res.* 20, 2029–2044. doi: 10.1016/S0278-4343(00)00055-8
- Shih, Y. Y., Hsieh, J. S., Gong, G. C., Chou, W. C., Lee, M. A., Hung, C. C., et al. (2013). Field observations of changes in SST, chlorophyll and POC flux in the southern East China Sea before and after the passage of typhoon Jangmi. *Terr. Atmos. Ocean. Sci.* 24, 899–910. doi: 10.3319/TAO.2013.05.23.01(Oc)
- Shih, Y. Y., Hung, C. C., Gong, G. C., Chung, W. C., Wang, Y. H., Lee, I. H., et al. (2015). Enhanced particulate organic carbon export at eddy edges in the oligotrophic western north Pacific Ocean. *PLoS One* 10:e0131538. doi: 10.1371/journal.pone.0131538
- Shih, Y. Y., Lin, H. H., Li, D., Hsieh, H. H., Hung, C. C., and Chen, C. T. A. (2019). Elevated carbon flux in deep waters of the South China Sea. *Sci. Rep.* 9:1496. doi: 10.1038/s41598-018-37726-w
- Siswanto, E., Ishizaka, J., Yokouchi, K., Tanaka, K., and Tan, C. K. (2007). Estimation of interannual and interdecadal variations of typhoon-induced primary production: a case study for the outer shelf of the East China Sea. *Geophys. Res. Lett.* 34:L03604. doi: 10.1029/2006gl028368
- Stewart, R. I. A., Dossena, M., Bohan, D. A., Jeppesen, E., Kordas, R. L., Ledger, M. E., et al. (2013). Mesocosm experiments as a tool for ecological climate change research. *Adv. Ecol. Res.* 48, 71–181. doi: 10.1016/B978-0-12-417199-2.00002-1
- Sweeney, E. N., McGillicuddy, D. J. Jr., and Buesseler, K. O. (2003). Biogeochemical impacts due to mesoscale eddy activity in the Sargasso Sea as measured at the Bermuda Atlantic Time-series Study (BATS). *Deep Sea Res. II* 50, 3017–3039. doi: 10.1016/j.dsr2.2003.07.008
- Tseng, C. M., Wong, G. T. F., Lin, I. I., Wu, C. R., and Liu, K. K. (2005). A unique seasonal pattern in phytoplankton biomass in low-latitude waters in the South China Sea. *Geophys. Res. Lett.* 32:L086080. doi: 10.1029/2004gl022111
- Zhao, H., Shao, J., Han, G., Yang, D., and Lv, J. (2015). Influence of typhoon Matsa on phytoplankton chlorophyll-a off East China. *PLoS One* 10:e0137863. doi: 10.1371/journal.pone.0137863
- Zhao, H., Tang, D. L., and Wang, Y. (2008). Comparison of phytoplankton blooms triggered by two typhoons with different intensities and translation speeds in the South China Sea. *Mar. Ecol. Prog. Ser.* 365, 57–65. doi: 10.3354/meps07488
- Zheng, G. M., and Tang, D. L. (2007). Offshore and nearshore chlorophyll increases induced by typhoon winds and subsequent terrestrial rainwater runoff. *Mar. Ecol. Prog. Ser.* 333, 61–74. doi: 10.3354/meps333061

Conflict of Interest: The authors declare that the research was conducted in the absence of any commercial or financial relationships that could be construed as a potential conflict of interest.

Copyright © 2020 Shih, Hung, Huang, Muller and Chen. This is an open-access article distributed under the terms of the Creative Commons Attribution License (CC BY). The use, distribution or reproduction in other forums is permitted, provided the original author(s) and the copyright owner(s) are credited and that the original publication in this journal is cited, in accordance with accepted academic practice. No use, distribution or reproduction is permitted which does not comply with these terms.